Polyomavirus-positive Merkel cell carcinoma derived from a trichoblastoma suggests an epithelial origin of this Merkel cell carcinoma

Thibault Kervarrec, Mohanad Aljundi, Silke Appenzeller, Mahtab Samimi, Eve Maubec, Bernard Cribier, Lydia Deschamps, Bhavishya Sarma, Eva-Maria Sarosi, Patricia Berthon, et al.

▶ **To cite this version:**

Thibault Kervarrec, Mohanad Aljundi, Silke Appenzeller, Mahtab Samimi, Eve Maubec, et al.. Polyomavirus-positive Merkel cell carcinoma derived from a trichoblastoma suggests an epithelial origin of this Merkel cell carcinoma. Journal of Investigative Dermatology, 2020, 140 (5), pp.976-985. 10.1016/j.jid.2019.09.026 . hal-02621965

HAL Id: hal-02621965
https://hal.inrae.fr/hal-02621965

Submitted on 20 May 2022

HAL is a multi-disciplinary open access archive for the deposit and dissemination of scientific research documents, whether they are published or not. The documents may come from teaching and research institutions in France or abroad, or from public or private research centers.

L'archive ouverte pluridisciplinaire **HAL**, est destinée au dépôt et à la diffusion de documents scientifiques de niveau recherche, publiés ou non, émanant des établissements d'enseignement et de recherche français ou étrangers, des laboratoires publics ou privés.

Distributed under a Creative Commons Attribution - NonCommercial 4.0 International License

Version of Record: https://www.sciencedirect.com/science/article/pii/S0022202X19333871
Manuscript_631af1d353f57500e51681ccd6a885f1

Polyomavirus-positive Merkel cell carcinoma derived from a trichoblastoma suggests an epithelial origin of this Merkel cell carcinoma

Thibault Kervarrec[1,2,3*,**], Mohanad Aljundi[4**], Silke Appenzeller[5**], Mahtab Samimi[2,6], Eve Maubec[4], Bernard Cribier[7], Lydia Deschamps[8], Bhavishya Sarma[3], Eva-Maria Sarosi[3], Patricia Berthon[2], Annie Levy[9], Guilhem Bousquet[10], Anne Tallet[11], Antoine Touzé[2], Serge Guyétant[1,2], David Schrama[3***] & Roland Houben[3***]

(1) Department of Pathology, Université de Tours, Centre Hospitalier Universitaire de Tours, 37044 Tours Cedex 09, France
(2) "Biologie des infections à polyomavirus" team, UMR INRA ISP 1282, Université de Tours,31, Avenue Monge 37200 TOURS, France
(3) Department of Dermatology, Venereology and Allergology, University Hospital Würzburg, Josef-Schneider-Straße 2, 97080 Würzburg, Germany
(4) Department of Dermatology, Avicenne University Hospital, 125 rue de Stalingrad, 97000 Bobigny, France
(5) Core Unit Bioinformatics, Comprehensive Cancer Center Mainfranken, University Hospital of Würzburg, Josef-Schneider-Straße 6, 97080 Würzburg, Germany
(6) Departement of Dermatology, Université de Tours, Centre Hospitalier Universitaire de Tours, 37044 Tours Cedex 09, France
(7) Dermatology Clinic, Hôpitaux Universitaires & Université de Strasbourg, Hôpital Civil, 1 Place de l'Hôpital, 67000 Strasbourg, France
(8) Department of Pathology Bichat Hospital, 45 rue Henri Huchard, 75018 Paris, France
(9) Department of Pathology, Avicenne University Hospital, 125 rue de Stalingrad, 97000 Bobigny, France
(10) Department of Medical Oncology, Avicenne University Hospital, 125 rue de Stalingrad, 97000 Bobigny, France
(11) Platform of Somatic Tumor Molecular Genetics, Université de Tours, Centre Hospitalier Universitaire de Tours, 37044 Tours Cedex 09, France

Disclosure/Conflict of Interest: The authors declare no conflict of interest.

(*) T. Kervarrec is the corresponding author. (**) T. Kervarrec, M. Aljundi and S. Appenzeller contributed equally to the present study. (***) D. Schrama and R. Houben contributed equally to the present study.

Grant numbers and sources of support: Fondation ARC pour la recherche contre le cancer, Interdisziplinäres Zentrum für Klinische Forschung Würzburg (IZKF B-343) and LEO Foundation Award to DS. Ligue nationale contre le cancer, Comités 16, 18, 28.

Institutional review board: The local Ethics Committee of Tours (France) approved the study (no. RCB2009-A01056-51)

Corresponding author:
Dr Thibault Kervarrec
Department of Pathology, Hôpital Trousseau, CHRU de Tours, 37044 TOURS Cedex 09
France. Tel: +33 (2) 47 47 80 69/Fax: +33 (2) 47 47 46 22
Email: thibaultkervarrec@yahoo.fr

Word count (Excluding abstract and references): 3552
List of attachments: Figures: 4 / Supplements consisting of 5 Tables, 4 Figures and 3 Supplementary Materials)

ORCID : Thibault Kervarrec: https://orcid.org/0000-0002-2201-6914 ; Mohanad Aljundi: https://orcid.org/0000-0002-6623-3267 ; Silke Appenzeller: https://orcid.org/0000-0002-5472-8692 ; Mahtab Samimi: https://orcid.org/0000-0001-6742-9088 ; Eve Maubec: https://orcid.org/0000-0003-1658-6686 ; Bernard Cribier: https://orcid.org/0000-0002-6306-770X; Lydia Deschamps: https://orcid.org/0000-0003-1468-8646 ; Bhavishya Sarma: https://orcid.org/0000-0002-1262-4721 ; Eva-Maria Sarosi: https://orcid.org/0000-0001-5075-4685 ; Patricia Berthon: https://orcid.org/0000-0002-3491-7613 ; Annie Levy: https://orcid.org/0000-0003-1468-8646 ; Guilhem Bousquet: https://orcid.org/0000-0001-5594-6694 ; Anne Tallet: https://orcid.org/0000-0002-2601-2443 ; Antoine Touzé: https://orcid.org/0000-0002-9856-9945 ; Serge Guyétant: https://orcid.org/0000-0003-2783-9722; David Schrama: https://orcid.org/0000-0002-6931-8194 ; Roland Houben: https://orcid.org/0000-0003-4538-2324

© 2019 published by Elsevier. This manuscript is made available under the CC BY NC user license
https://creativecommons.org/licenses/by-nc/4.0/

Abstract

Merkel cell carcinoma (MCC), an aggressive neuroendocrine carcinoma of the skin, is to date the only human cancer known to be frequently caused by a polyomavirus. However, it is a matter of debate which cells are targeted by the Merkel cell polyomavirus (MCPyV) to give rise to the phenotypically multifaceted MCC cells.

To assess the lineage of origin of MCPyV-positive MCC, genetic analysis of a very rare tumor combining benign trichoblastoma and MCPyV-positive MCC was conducted by massive parallel sequencing. Although MCPyV was found to be integrated only in the MCC part, six somatic mutations were shared by both tumor components. The mutational overlap between trichoblastoma and MCPyV-positive MCC part of the combined tumor implies that MCPyV integration occurred in an epithelial tumor cell prior to MCC development. Therefore, our report demonstrates that MCPyV-positive MCC can derive from the epithelial lineage.

Introduction

Merkel cell carcinoma (MCC) is a rare, aggressive neoplasm of the skin with a 5-year overall survival rate of 40% (Becker et al. 2017). In about 80% of MCC cases the Merkel cell polyomavirus (MCPyV), an ubiquitous virus causing asymptomatic infections in the general population, is integrated into the genome of the tumor cells (Feng et al. 2008). In addition to the random integration of MCPyV, alterations of the viral sequence resulting in a truncated Large T antigen (LT) devoid of replicative abilities seem to be essential for MCC oncogenesis. Together with the truncated LT a viral small T antigen (sT) with multiple oncogenic properties is expressed in MCC cells, and both oncoproteins are considered as the main drivers for development and growth of MCPyV-positive MCC (Becker et al. 2017).

Although it is well established that MCPyV is a crucial oncogenic trigger in MCC pathogenesis, the nature of the cell in which virus integration occurs is unknown. Despite close phenotypic similarities with MCC such as expression of keratin (KRT) 20 and neuroendocrine markers, the eponym Merkel cell (MC) is considered as an unlikely candidate because this mechanoreceptor cell is post-mitotic (Van Keymeulen et al. 2009), insensitive to oncogenic stimuli in mice (Shuda et al. 2015), and - while MCCs are predominantly dermal or hypodermal (Pulitzer 2017) - resides in the basal layer of the epidermis (Halata et al. 2003). Alternatively, MCPyV integration could occur in a non-MC, and an MC-like phenotype might be acquired during tumorigenesis (Sunshine et al. 2018). In this respect, epithelial, fibroblastic, lymphoid as well as a neural crest origin of MCC have been discussed as potential candidates for MCC origin (Liu et al. 2016; Sunshine et al. 2018; Tilling and Moll 2012; Zur Hausen et al. 2013). Here, analysis of a rare combined tumor consisting of trichoblastoma and MCC parts, suggests that an MCPyV-positive MCC can arise from an epithelial cell.

Results

An MCPyV-positive MCC within a benign epithelial follicular tumor

In this study, a case of combined trichoblastoma/MCC tumor was subjected to extensive analyses. Details of the case are available in **Supplementary Table S1** and **Supplementary Figures S1-2**. Briefly, morphological examination revealed a well-delimitated tumor located in the subcutis, without connection to the epidermis and harboring two different components **(Figure 1a and b)**. On the borders, the combined tumor displayed typical trichoblastoma features with epithelial follicular germinative cells arranged in nodules or anastomotic strands entrapped in a prototypic stroma mimicking the dermal papillae **(Figure 1a-b** and **Supplementary Figure S1)**. By contrast, the MCC part, located in the center of the combined tumor, was composed of sheets of round, medium-sized tumor cells with scant cytoplasm, round nucleus and dusty clear chromatin **(Figure 1a-b)**. Immunohistochemical investigations **(Figure 1c-e/Supplementary Figure S2)** confirmed the diagnosis, notably revealing co-expression of KRT20 and neuroendocrine markers in all MCC cells and scattered KRT20-positive MCs in the trichoblastoma, a hallmark of this entity (Kurzen et al. 2001).

It has been suggested that MCPyV is not involved in the development of combined MCCs (Martin et al. 2013) which account for 5-10% of all MCCs (Kervarrec et al. 2018a). However, quantitative PCR demonstrated a substantial MCPyV viral load (20 copies/cell) in the MCC component, and staining for MCPyV-LT (**Figure 1c)** revealed moderate expression in the MCC cells suggesting an MCPyV-driven oncogenesis. In contrast, most of the trichoblastoma stained negative, and only in one restricted area a fraction of cells expressed LT (**Figure 1c**). It could, however, not be concluded whether these cells represented MCPyV-infected trichoblastoma cells or disseminated cells from the adjacent MCC tumor **(Figure 1b)**. Interestingly, an increased number of cells expressing the MC differentiation markers SOX2,

KRT8 and KRT20 was present in this area, with KRT8 and KRT20 frequently displaying a distinct paranuclear dot-like pattern dissimilar from the diffuse cytoplasmic KRT20-distribution in normal MCs in the rest of the trichoblastoma component (**Figure 1d-e/Supplementary Figure S3a-c**). Furthermore, co-expression of KRT20 and LT in about 50% and KRT20 and the proliferation marker MKi67 in about 10% of the KRT20-expressing cells was observed (**Supplementary Figure S3a, c-d**).

In summary, the morphological and immunohistochemical analyses of the combined tumor revealed presence of MCPyV in specific trichoblastoma areas and widespread presence of MCPyV in the MCC part suggesting a virus-induced MCC oncogenesis.

MCPyV integration and LT truncation in the MCC

Two molecular features characterize MCPyV-associated MCC. First, the virus genome is clonally integrated into the genome of the tumor cells (Feng et al. 2008) and second, the LT antigen coding sequence is always affected in a way leading to expression of a truncated protein (Shuda et al. 2008). Applying combination of whole genome and Sanger sequencing onto DNA isolated from the MCC part, we could detect and confirm integration of MCPyV in chromosome 3 of the tumor genome (**Figure 2a-b**). Moreover, the presence of MCPyV sequences beyond the unique break points suggest integration of a concatemer consisting of one or more viral copies in addition to the sequence between the break points. Sequencing further indicates that even two differently truncated LT proteins may be expressed in the MCC part. One truncation caused by the integration break point at 1956, the other by a deletion spanning base pairs 2248 – 2542 (both according to GenBank EU375803) (**Fig. 2b**). In conclusion, the genetic analysis of MCPyV in the MCC part of the combined tumor revealed that this carcinoma harbors the hallmarks of an MCPyV-positive MCC.

Importantly, amplification of the insertion sites and a fragment specific for the LT-truncating deletion was only achieved with DNA from the MCC while from the trichoblastoma DNA only wild type LT sequence could be amplified **(Figure 2c)**. These results clearly indicate that the trichoblastoma tumor cells do not harbor the integrated form of the virus found in the MCC.

Shared mutations in trichoblastoma and MCC component

In order to prove a genetic relationship between the MCPyV-positive MCC and the trichoblastoma part of the combined tumor, DNA isolated from the different tumor components and healthy tissue was analyzed by whole exome sequencing and somatic mutations were identified **(Supplementary Tables S2-4)**. Several acquired variants were present in only one of the tumor samples indicating that each tumor component partly experienced its own genetic history. Strikingly, however, the six acquired non-synonymous variants detected with the highest allelic frequencies in the trichoblastoma were also present in the MCC part **(Supplementary Table S2**). This was confirmed by Sanger sequencing (**Figure 3**) thus suggesting a common origin of the two tumor parts. Since integrated MCPyV could only be detected in the MCC part **(Fig. 2c)**, these results imply that upon MCPyV integration occurring in an epithelial cell of the trichoblastoma component the MCC developed. In line with this, allelic frequencies of approximately 50% for the shared somatic mutations in the MCC part (lacking significant stroma **(Figure 1)**) are in accordance with heterozygous mutations being present in all MCC tumor cells. Measured allelic frequencies of 21-32% in the trichoblastoma part **(Figure 3 and Supplementary Table S2)**, which harbors more extensive stroma **(Figure 1**), may reflect heterozygotic presence of the shared mutations in most if not all trichoblastoma cells. Interestingly, all further mutations detected in the trichoblastoma part were less frequent **(Supplementary Table S2)** suggesting that they are

not present in all trichoblastoma cells. This is in line with a scenario where MCPyV integration has occurred in a trichoblastoma cell lacking these mutations. Among the somatic variants present in only the MCC part there are some which were detected with frequencies close to those of the shared mutations (e.g. GRIK4 and FAM219A) **(Supplementary Table S2).** They either may represent (i) mutations, present below the detection limit in the trichoblastoma but, nevertheless existent in the specific "MCC cell of origin", or (ii) may have been acquired early during MCPyV-mediated oncogenesis. Finally, the low number of mutations lacking any UV-signature **(Supplementary Table S4)** confirms that the MCC part of the combined tumor matches also these attributes of MCPyV-positive MCC (Becker et al. 2017).

In conclusion, the data provided so far, clearly indicate that an MCPyV-positive MCC can arise from an epithelial cell.

Analogy between trichoblastoma and MC progenitor

Next, we asked whether the analyses of the combined tumor would allow further conclusions regarding the cellular origin of this MCPyV-positive MCC. As expected, an epithelial lineage descendance was confirmed by widespread expression of cytokeratins in trichoblastoma cells. Moreover, trichoblastoma cells characteristically bear intrinsic MC-differentiation capability and phenotypically resemble hair follicle stem cells (Kurzen et al. 2001) (**Figure 4a-c**) which have been demonstrated to be essential for MC development (Nguyen et al. 2018; Perdigoto et al. 2016). In particular, GLI1 activation in the hair follicle and the surrounding touch domes is critical for the maintenance of the MC lineage (Perdigoto et al. 2016; Xiao et al. 2015). Interestingly, we could demonstrate in the trichoblastoma part of the combined tumor, like in normal hair follicles, widespread expression of KRT17 and SOX9, two markers shared by hair follicle and MC-progenitors as well as GLI1 nuclear localization **(Figure 4c-e)** (Brownell et al. 2011; Larouche et al. 2008; Moll et al. 1993; Nguyen et al. 2018; Nguyen et al. 2018;

Xiao et al. 2015) in association with the interspersed presence of KRT8-and KRT20-positive MCs **(Figures 1c and 4f, Supplementary Figure S3b-d)**. Therefore, the trichoblastoma cell in which MCPyV integration occurred as demonstrated by genomic analyses could be either a cell resembling an epithelial progenitor cell of the hair follicle or an already differentiated MC.

A second case of MCPyV-positive MCC arising within a trichoblastoma

Our study has limitations and most prominent, our conclusions are based on only one case. Due to the exceedingly low incidence of combined trichoblastoma/MCC, we could identify only one additional case published previously (Battistella et al. 2011). Analyses of this second combined MCC by immunohistochemistry confirmed a further case of MCPyV-positive MCC arising within a trichoblastoma composed of KRT17- and SOX9-positive MC-precursor-like cells and interspersed KRT20- and KRT-8 expressing MCs (**Supplementary Figure S4/Supplementary Table S5**). Unfortunately, additional molecular analyses could not be performed due to very poor DNA quality related to Bouin fixation.

Discussion

Identification of the cellular origin of MCPyV-positive and virus-negative MCC are considered as high-priority research questions not only to improve our understanding of the initiation of this disease, but also for developing appropriate models and possibly new therapeutic approaches (Harms et al. 2018; Sauer et al. 2017; Sunshine et al. 2018). Due to close phenotypic similarities with MCC, MC – a highly specialized mechanoreceptor, and a descendant from KRT14-positive epidermal progenitors (Halata et al. 2003; Van Keymeulen et al. 2009) - was historically regarded as the cell of origin of MCC. Proposed alternatives as potential MCC origin include pre/pro-B cells, dermal fibroblasts, dermal mesenchymal stem cells and epithelial progenitor cells (Becker and Zur Hausen 2014; Kervarrec et al. 2019; Lemasson et al. 2012; Liu et al. 2016; Tilling and Moll 2012; Verhaegen et al. 2017; Woo et al. 2010; Zur Hausen et al. 2013).

Although investigating only a single case belonging to an exceptionally rare tumor entity, the results presented here provide a clear proof that MCPyV-positive MCC can arise from the epithelial lineage, i.e., either from already differentiated MCs or their progenitors. Moreover, while an alternative histogenesis either in mesenchymal or lymphoid cells could not formerly be excluded for other MCPyV-positive MCC cases such scenario appears unlikely because a tumor cell phenotype is determined by both, the tumorigenic alterations and by the primary nature of the cell of origin ' (Bailleul et al. 1990; Brown et al. 1998; Visvader 2011). This concept referred to as "oncogene lineage-addiction" (Garraway and Sellers 2006) was proven for MCPyV oncoproteins using transgenic mice. Indeed, in such model, ectopic expression of the T antigens (sT alone or in combination with LT) failed to generate tumors with an MCC-like phenotype in all tested compartments (Shuda et al. 2015; Spurgeon et al. 2015; Verhaegen et al. 2015) except for the Merkel cell lineage (Verhaegen et al. 2017). In light of

these findings, while trichoblastoma tumors could not be considered as a frequent site of MCPyV integration, it is conceivable that MCPyV induced carcinogenesis occurs in a similar cellular context i.e. an epithelial cell of the MC lineage being either an hair follicle progenitor or an already differentiated MC.

Indeed, we confirmed trichoblastoma as a benign epithelial tumor phenotypically resembling progenitor cells of the hair follicle (Kurzen et al. 2001) and bearing MC differentiation ability (Katona et al. 2008; Kurzen et al. 2001; Leblebici et al. 2018). Under physiological conditions, the hair follicle is a privileged niche for MC differentiation and accordingly, abrogation of hair follicle development in transgenic mice resulted in complete MC loss (Perdigoto et al. 2016). Furthermore, Sox9- and Fgfr2-expressing cells in the embryonic hair follicle were identified as MC progenitors, and active Sonic hedgehog signaling was shown to be critical for establishment of this population , and for subsequent MC differentiation (Nguyen et al. 2018; Perdigoto et al. 2016). Interestingly, all these features can also be found in the trichoblastoma germinative cells of the presented combined tumor and accordingly sparse MCs were detected. Therefore our results suggest that hair follicles with potential for MC differentiation might represent a major cellular origin of MCPyV-positive MCC. This notion has been suggested earlier (Tilling and Moll 2012), and is also corroborated by rare cases of MCC found within follicular cysts (Requena et al. 2008; Su et al. 2008). Furthermore, frequent connections between MCC tumors and hair follicles have been described (Walsh 2001) although one might also argue that collision with a hair follicle is an inevitable consequence when a dermal tumor reaches a certain size.

Of note, while the lineage from which tumor cells derived have been identified for several solid cancers, the precise differentiation degree of the cell in which transformation occurs

remains elusive in most cases (Visvader 2011). In the analyzed tumor, oncogenic virus integration may have occurred in one of the differentiated MCs present in the trichoblastoma. On the other hand, arguments against the possibility that MCCs arise from already differentiated MCs include i) lack of mitotic activity of MCs (Moll et al. 1996), although a recent publication demonstrated some proliferative activity (Narisawa et al. 2019), ii) poor MCPyV infectibility (Liu et al. 2016) and iii) insusceptibility of these cells to oncogenic stimuli (including T antigens) in mice (Shuda et al. 2015; Van Keymeulen et al. 2009). Alternatively, MCC could derive from MC progenitors (Tilling and Moll 2012) which can arise from GLI1-expressing hair follicle stem cells. Interestingly, this population has been demonstrated to be highly susceptible to tumorigenic stimuli, and can serve as an important cellular origin in the development of other skin cancers (Peterson et al. 2015). In such a scenario phenotypic changes may arise during oncogenesis (Fletcher 2006). In this regard, it has been suggested that TA expression can induce an MC-like differentiation process (Sunshine et al. 2018). Indeed, expression of LT of the polyomavirus simian virus 40 in gastric or prostate murine epithelial cells can induce an epithelial to neuroendocrine differentiation (Kaplan-Lefko et al. 2003; Syder et al. 2004). Moreover, in human prostate cancer as well as mouse models, inactivation of RB1 and TP53 – both expected outcomes of MCPyV-TA expression (Houben et al. 2012; Park et al. 2019) – have been demonstrated to induce the epigenetic reprogramming factors SOX2 and EZH2 (Ku et al. 2017), i.e. two critical actors involved in Merkel cell differentiation. In line with these published results, we observed an increase in cells positive for the MC markers KRT8, SOX2 and KRT20 in a trichoblastoma region containing MCPyV-LT expression. Although a metastatic spreading of the MCC tumor cells with “small cell morphology” into the trichoblastoma might explain these findings, it could alternatively be the result of LT-induced MC proliferation, or indicate a differentiation process promoted by MCPyV oncoproteins. This notion is supported by more

frequent cells expressing SOX2 and KRT8 which appear earlier during MC differentiation than the less frequently expressed KRT20 (**Supplementary Figure 3**) (Perdigoto et al. 2014). Taken together, it is conceivable that MCPyV-TAs contribute to the development of a MC-like phenotype upon expression in an epithelial precursor cell.

Irrespective of these more speculative considerations, the mutational overlap between a benign epithelial tumor and a MCPyV-positive MCC provides a clear proof that an MCPyV-positive MCC can evolve from an epithelial cell. Moreover, close similarities between trichoblastoma and MC progenitors suggest that cells of the MC lineage might represent a prominent cellular target of MCPyV in MCC carcinogenesis.

Methods

Ethics

This study was approved by the local ethics committee (Tours, France, N° ID RCB2009-A01056-51), and written, informed consent of the patient was obtained.

Immunochemistry

Immunohistochemical staining for CD274, CHGA, pan-KRT (AE1/AE3), KRT14, KRT20, MKI67, MCPyV-LT, TP53, SOX9, TDT and TTF1 as well as double staining for KRT20/MCPyV-LT and KRT/MKI67 was performed using a BenchMark XT Platform as instructed (Kervarrec et al. 2018b; Kervarrec et al. 2018a). Immunohistochemical staining for GLI1, KRT8, KRT15, KRT17 and SOX2 was performed manually. Antibodies and dilutions are provided in **Supplementary Materials**. TP53 as well as MCPyV-LT were analyzed using an Allred score (Moshiri et al. 2016). Quantification of LT, KRT8 and -20, SOX2 and MKI67 positive cells in MCPyV(+) and (-) trichoblastoma areas was performed by counting cells in 8 independent fields (0.027 mm^2) and compared using a Mann-Whitney test.

DNA isolation and MCPyV quantitative PCR

After microdissection of the two tumor components and of the healthy tissue under a binocular magnifier, genomic DNA was isolated by use of the Maxwell 16 Instrument (Promega) with the Maxwell 16 formalin-fixed and paraffin-embedded Plus LEV DNA purification kit (Promega). MCPyV-LT real-time PCR was performed as described (Kervarrec et al. 2018b). Of note, dissection of the trichoblastoma was performed in areas devoid of LT expression. Briefly, 50 ng DNA was mixed with primers (0.2 µM), probe (0.1 µM) and Mix Life technologies GoTaq Probe real-time PCR Master Mix 2X (Promega) in a final volume of 20 µl. PCR reactions were performed with the LightCycler 480 II (Roche) with an initial denaturation at 95°C × 2 min, followed by 45 cycles at 95°C × 15 sec and 58°C × 60 sec. Albumin was used as reference gene for normalization. The $2^{-\Delta Ct}$ method was used

for quantification, and results expressed as number of MCPyV copies per cell (Kervarrec et al. 2018b). Sequences of the primers used for quantitative PCR are available in **Supplementary Materials**.

PCR amplification and Sanger sequencing.

Nested PCRs with primers listed in **Supplementary Materials** were performed to amplify the respective regions. PCR reactions were carried out in a total volume of 20 µl containing 1x HF buffer, 1 µM of each primer, 200 µM dNTPs, 1 unit Q5 Phusion (NEB) and 1 µl of template. After an initial denaturation at 98°C for 1 min, the thermal profile consisted of denaturation at 98°C for 10 sec, annealing at the optimal temperature for 30 sec and elongation at 72°C for 1 min (30 cycles for pre-amplification and 40 cycles for amplification). After PCR purification the amplicons were sent to Seqlab (Microsynth) for sequencing.

Next Generation Sequencing

For the library preparation of the exomes the SureSelectXT Library Prep Kit (Agilent) was used. Enrichment was performed using Agilent's SureSelectXT Human All Exon V6 Kit. The genomic library was prepared using TruSeq Nano DNA (Illumina). Paired end sequencing with a read length of 100 bps (exomes) and 150 bps (genome) was performed on a NovaSeq 6000 (Illumina).

Data analysis

Demultiplexing of the sequencing reads was performed with Illumina bcl2fastq (v2.19). Adapters were trimmed with Skewer, v0.2.25 (Jiang et al. 2014). An initial quality assessment was performed using FastQC, v0.11.5 (Andrews S., 2010. Available online at: http://www.bioinformatics.babraham.ac.uk/projects/fastqc). Low-quality reads were trimmed with TrimGalore, v0.4.0 (Krueger, F., 2012: Available online at: http://www.bioinformatics.babraham.ac.uk/projects/trim_galore/) powered by Cutadapt, v1.86

(Martin 2011). The trimmed reads were mapped to the human reference genome (hg19) using BWA mem, v0.7.127 (Li and Durbin 2009) and sorted and indexed using Picard, v1.125 (available online at: http://broadinstitute.github.io/picard/) and SAMtools, v1.38 (Li et al. 2009) respectively. Duplicates were marked with Picard. For the exomes local realignment around indels was executed with GATK, v3.59 (McKenna et al. 2010). GATK was also used for coverage calculations.

Somatic variant calling

MuTect1, v 1.1.410 (Cibulskis et al. 2013) and VarScan2, v2.4.111(Koboldt et al. 2012) were used to identify somatic single nucleotide variants (SNVs). Samtools (mpileup) with VarScan2 and Scalpel, v0.5.312 (Fang et al. 2016) were applied to identify small somatic insertions or deletions. All variants were annotated with ANNOVAR, v2017-06-0113 (Wang et al. 2010). Six somatic variants shared by the trichoblastoma and the MCC were visually examined using the Integrative Genomics Viewer, v2.3.6814 (Thorvaldsdóttir et al. 2013) and confirmed with Sanger sequencing if they have an impact on the protein sequence or affect a splice site, are rare in the population (below a frequency of 2 % in 1000g2015aug_all, ExAC_nontcga_ALL, gnomAD_exome_ALL and gnomAD_genome_ALL) and the position is covered by at least 20 reads and the alternative allele is covered by at least 8 reads and comprised at least 5 %. Mutational signatures were identified using MuSiCa (Díaz-Gay et al. 2018) investigating somatic variants comprised at least 10%.

Detection of the virus integration site

Seeksv, v1.2.315 (Liang et al. 2017) was used with the human reference genome sequence (hg19) and the MCPyV MCC350 genome sequence (GenBank EU375803) to detect the virus integration site.

Data availability statement

The datasets generated during and/or analysed during the current study are available in European Genome-phenome Archive (ID: EGAS00001003784).

Acknowledgements

The authors thank Dr A. Balaton, Dr L. Durand, Dr J Mabille and Dr S. Manela for their help and contribution.

Competing interests

The authors declare no competing interests.

Contributions

Design of the study: TK, DS, R.H; Data acquisition and analysis and interpretation: TK, DS, RH, MA, SA, MS, EM, BC, SG, LD, BS, PB, AL, EMS, AT, GB, AT; Manuscript writing: TK, DS, RH; Revision of the manuscript: TK, DS, RH, MA, SA, MS, EM, BC, SG, LD, BS, PB, AL, EMS, AT, GB, AT.

Corresponding author

Correspondence to Thibault Kervarrec.

References

Bailleul B, Surani MA, White S, Barton SC, Brown K, Blessing M, et al. Skin hyperkeratosis and papilloma formation in transgenic mice expressing a ras oncogene from a suprabasal keratin promoter. Cell. 1990;62(4):697–708

Battistella M, Durand L, Jouary T, Peltre B, Cribier B. Primary cutaneous neuroendocrine carcinoma within a cystic trichoblastoma: a nonfortuitous association? Am. J. Dermatopathol. 2011;33(4):383–7

Becker JC, Stang A, DeCaprio JA, Cerroni L, Lebbé C, Veness M, et al. Merkel cell carcinoma. Nat. Rev. Dis. Primer. 2017;3:17077

Becker JC, Zur Hausen A. Cells of origin in skin cancer. J. Invest. Dermatol. 2014;134(10):2491–3

Brown K, Strathdee D, Bryson S, Lambie W, Balmain A. The malignant capacity of skin tumours induced by expression of a mutant H-ras transgene depends on the cell type targeted. Curr. Biol. CB. 1998;8(9):516–24

Brownell I, Guevara E, Bai CB, Loomis CA, Joyner AL. Nerve-derived sonic hedgehog defines a niche for hair follicle stem cells capable of becoming epidermal stem cells. Cell Stem Cell. 2011;8(5):552–65

Cibulskis K, Lawrence MS, Carter SL, Sivachenko A, Jaffe D, Sougnez C, et al. Sensitive detection of somatic point mutations in impure and heterogeneous cancer samples. Nat. Biotechnol. 2013;31(3):213–9

Díaz-Gay M, Vila-Casadesús M, Franch-Expósito S, Hernández-Illán E, Lozano JJ, Castellví-Bel S. Mutational Signatures in Cancer (MuSiCa): a web application to implement mutational signatures analysis in cancer samples. BMC Bioinformatics. 2018;19(1):224

Fang H, Bergmann EA, Arora K, Vacic V, Zody MC, Iossifov I, et al. Indel variant analysis of short-read sequencing data with Scalpel. Nat. Protoc. 2016;11(12):2529–48

Feng H, Shuda M, Chang Y, Moore PS. Clonal integration of a polyomavirus in human Merkel cell carcinoma. Science. 2008;319(5866):1096–100

Fletcher CDM. The evolving classification of soft tissue tumours: an update based on the new WHO classification. Histopathology. 2006;48(1):3–12

Garraway LA, Sellers WR. Lineage dependency and lineage-survival oncogenes in human cancer. Nat. Rev. Cancer. 2006;6(8):593–602

Halata Z, Grim M, Bauman KI. Friedrich Sigmund Merkel and his “Merkel cell”, morphology, development, and physiology: review and new results. Anat. Rec. A. Discov. Mol. Cell. Evol. Biol. 2003;271(1):225–39

Harms PW, Harms KL, Moore PS, DeCaprio JA, Nghiem P, Wong MKK, et al. The biology and treatment of Merkel cell carcinoma: current understanding and research priorities. Nat. Rev. Clin. Oncol. 2018;

Houben R, Adam C, Baeurle A, Hesbacher S, Grimm J, Angermeyer S, et al. An intact retinoblastoma protein-binding site in Merkel cell polyomavirus large T antigen is required for promoting growth of Merkel cell carcinoma cells. Int. J. Cancer. 2012;130(4):847–56

Iwasaki T, Kodama H, Matsushita M, Kuroda N, Yamasaki Y, Murakami I, et al. Merkel cell polyomavirus infection in both components of a combined Merkel cell carcinoma and basal cell carcinoma with ductal differentiation; each component had a similar but different novel Merkel cell polyomavirus large T antigen truncating mutation. Hum. Pathol. 2013;44(3):442–7

Jiang H, Lei R, Ding S-W, Zhu S. Skewer: a fast and accurate adapter trimmer for next-generation sequencing paired-end reads. BMC Bioinformatics. 2014;15:182

Kaplan-Lefko PJ, Chen T-M, Ittmann MM, Barrios RJ, Ayala GE, Huss WJ, et al. Pathobiology of autochthonous prostate cancer in a pre-clinical transgenic mouse model. The

Prostate. 2003;55(3):219–37
Katona TM, Perkins SM, Billings SD. Does the panel of cytokeratin 20 and androgen receptor antibodies differentiate desmoplastic trichoepithelioma from morpheaform/infiltrative basal cell carcinoma? J. Cutan. Pathol. 2008;35(2):174–9
Kervarrec T, Samimi M, Gaboriaud P, Gheit T, Beby-Defaux A, Houben R, et al. Detection of the Merkel cell polyomavirus in the neuroendocrine component of combined Merkel cell carcinoma. Virchows Arch. Int. J. Pathol. 2018a;
Kervarrec T, Samimi M, Guyétant S, Sarma B, Chéret J, Blanchard E, et al. Histogenesis of Merkel cell carcinoma: a comprehensive review. Front. Oncol. Accepted Manuscript. 2019;
Kervarrec T, Tallet A, Miquelestorena-Standley E, Houben R, Schrama D, Gambichler T, et al. Diagnostic accuracy of a panel of immunohistochemical and molecular markers to distinguish Merkel cell carcinoma from other neuroendocrine carcinomas. Mod. Pathol. Off. J. U. S. Can. Acad. Pathol. Inc. 2018b;
Koboldt DC, Zhang Q, Larson DE, Shen D, McLellan MD, Lin L, et al. VarScan 2: somatic mutation and copy number alteration discovery in cancer by exome sequencing. Genome Res. 2012;22(3):568–76
Ku SY, Rosario S, Wang Y, Mu P, Seshadri M, Goodrich ZW, et al. Rb1 and Trp53 cooperate to suppress prostate cancer lineage plasticity, metastasis, and antiandrogen resistance. Science. 2017;355(6320):78–83
Kurzen H, Esposito L, Langbein L, Hartschuh W. Cytokeratins as markers of follicular differentiation: an immunohistochemical study of trichoblastoma and basal cell carcinoma. Am. J. Dermatopathol. 2001;23(6):501–9
Larouche D, Tong X, Fradette J, Coulombe PA, Germain L. Vibrissa hair bulge houses two populations of skin epithelial stem cells distinct by their keratin profile. FASEB J. Off. Publ. Fed. Am. Soc. Exp. Biol. 2008;22(5):1404–15
Leblebici C, Bambul Sığırcı B, Kelten Talu C, Koca SB, Huq GE. CD10, TDAG51, CK20, AR, INSM1, and Nestin Expression in the Differential Diagnosis of Trichoblastoma and Basal Cell Carcinoma. Int. J. Surg. Pathol. 2018;1066896918781719
Lemasson G, Coquart N, Lebonvallet N, Boulais N, Galibert MD, Marcorelles P, et al. Presence of putative stem cells in Merkel cell carcinomas. J. Eur. Acad. Dermatol. Venereol. JEADV. 2012;26(6):789–95
Li H, Durbin R. Fast and accurate short read alignment with Burrows-Wheeler transform. Bioinforma. Oxf. Engl. 2009;25(14):1754–60
Li H, Handsaker B, Wysoker A, Fennell T, Ruan J, Homer N, et al. The Sequence Alignment/Map format and SAMtools. Bioinforma. Oxf. Engl. 2009;25(16):2078–9
Liang Y, Qiu K, Liao B, Zhu W, Huang X, Li L, et al. Seeksv: an accurate tool for somatic structural variation and virus integration detection. Bioinforma. Oxf. Engl. 2017;33(2):184–91
Liu W, Yang R, Payne AS, Schowalter RM, Spurgeon ME, Lambert PF, et al. Identifying the Target Cells and Mechanisms of Merkel Cell Polyomavirus Infection. Cell Host Microbe. 2016;19(6):775–87
Martin M. Cutadapt removes adapter sequences from high-throughput sequencing reads. EMBnet.journal. 2011;17(1):10
Martin B, Poblet E, Rios JJ, Kazakov D, Kutzner H, Brenn T, et al. Merkel cell carcinoma with divergent differentiation: histopathological and immunohistochemical study of 15 cases with PCR analysis for Merkel cell polyomavirus. Histopathology. 2013;62(5):711–22
McKenna A, Hanna M, Banks E, Sivachenko A, Cibulskis K, Kernytsky A, et al. The Genome Analysis Toolkit: a MapReduce framework for analyzing next-generation DNA sequencing data. Genome Res. 2010;20(9):1297–303
Moll I, Troyanovsky SM, Moll R. Special program of differentiation expressed in

keratinocytes of human haarscheiben: an analysis of individual cytokeratin polypeptides. J. Invest. Dermatol. 1993;100(1):69–76
Moll I, Zieger W, Schmelz M. Proliferative Merkel cells were not detected in human skin. Arch. Dermatol. Res. 1996;288(4):184–7
Moshiri AS, Doumani R, Yelistratova L, Blom A, Lachance K, Shinohara MM, et al. Polyomavirus-Negative Merkel Cell Carcinoma: A More Aggressive Subtype Based on Analysis of 282 Cases Using Multimodal Tumor Virus Detection. J. Invest. Dermatol. 2016;
Narisawa Y, Inoue T, Nagase K. Evidence of proliferative activity in human Merkel cells: implications in the histogenesis of Merkel cell carcinoma. Arch. Dermatol. Res. 2019;311(1):37–43
Nguyen MB, Cohen I, Kumar V, Xu Z, Bar C, Dauber-Decker KL, et al. FGF signalling controls the specification of hair placode-derived SOX9 positive progenitors to Merkel cells. Nat. Commun. 2018;9(1):2333
Park DE, Cheng J, Berrios C, Montero J, Cortés-Cros M, Ferretti S, et al. Dual inhibition of MDM2 and MDM4 in virus-positive Merkel cell carcinoma enhances the p53 response. Proc. Natl. Acad. Sci. U. S. A. 2019;116(3):1027–32
Perdigoto CN, Bardot ES, Valdes VJ, Santoriello FJ, Ezhkova E. Embryonic maturation of epidermal Merkel cells is controlled by a redundant transcription factor network. Dev. Camb. Engl. 2014;141(24):4690–6
Perdigoto CN, Dauber KL, Bar C, Tsai P-C, Valdes VJ, Cohen I, et al. Polycomb-Mediated Repression and Sonic Hedgehog Signaling Interact to Regulate Merkel Cell Specification during Skin Development. PLoS Genet. 2016;12(7):e1006151
Peterson SC, Eberl M, Vagnozzi AN, Belkadi A, Veniaminova NA, Verhaegen ME, et al. Basal cell carcinoma preferentially arises from stem cells within hair follicle and mechanosensory niches. Cell Stem Cell. 2015;16(4):400–12
Pulitzer M. Merkel Cell Carcinoma. Surg. Pathol. Clin. 2017;10(2):399–408
Requena L, Jaqueti G, Rütten A, Mentzel T, Kutzner H. Merkel cell carcinoma within follicular cysts: report of two cases. J. Cutan. Pathol. 2008;35(12):1127–33
Sauer CM, Haugg AM, Chteinberg E, Rennspiess D, Winnepenninckx V, Speel E-J, et al. Reviewing the current evidence supporting early B-cells as the cellular origin of Merkel cell carcinoma. Crit. Rev. Oncol. Hematol. 2017;116:99–105
Shuda M, Feng H, Kwun HJ, Rosen ST, Gjoerup O, Moore PS, et al. T antigen mutations are a human tumor-specific signature for Merkel cell polyomavirus. Proc. Natl. Acad. Sci. U. S. A. 2008;105(42):16272–7
Shuda M, Guastafierro A, Geng X, Shuda Y, Ostrowski SM, Lukianov S, et al. Merkel Cell Polyomavirus Small T Antigen Induces Cancer and Embryonic Merkel Cell Proliferation in a Transgenic Mouse Model. PloS One. 2015;10(11):e0142329
Spurgeon ME, Cheng J, Bronson RT, Lambert PF, DeCaprio JA. Tumorigenic activity of merkel cell polyomavirus T antigens expressed in the stratified epithelium of mice. Cancer Res. 2015;75(6):1068–79
Su W, Kheir SM, Berberian B, Cockerell CJ. Merkel cell carcinoma in situ arising in a trichilemmal cyst: a case report and literature review. Am. J. Dermatopathol. 2008;30(5):458–61
Sunshine JC, Jahchan NS, Sage J, Choi J. Are there multiple cells of origin of Merkel cell carcinoma? Oncogene. 2018;
Syder AJ, Karam SM, Mills JC, Ippolito JE, Ansari HR, Farook V, et al. A transgenic mouse model of metastatic carcinoma involving transdifferentiation of a gastric epithelial lineage progenitor to a neuroendocrine phenotype. Proc. Natl. Acad. Sci. U. S. A. 2004;101(13):4471–6
Thorvaldsdóttir H, Robinson JT, Mesirov JP. Integrative Genomics Viewer (IGV): high-

performance genomics data visualization and exploration. Brief. Bioinform. 2013;14(2):178–92
Tilling T, Moll I. Which are the cells of origin in merkel cell carcinoma? J. Skin Cancer. 2012;2012:680410
Van Keymeulen A, Mascre G, Youseff KK, Harel I, Michaux C, De Geest N, et al. Epidermal progenitors give rise to Merkel cells during embryonic development and adult homeostasis. J. Cell Biol. 2009;187(1):91–100
Verhaegen ME, Mangelberger D, Harms PW, Eberl M, Wilbert DM, Meireles J, et al. Merkel Cell Polyomavirus Small T Antigen Initiates Merkel Cell Carcinoma-like Tumor Development in Mice. Cancer Res. 2017;77(12):3151–7
Verhaegen ME, Mangelberger D, Harms PW, Vozheiko TD, Weick JW, Wilbert DM, et al. Merkel cell polyomavirus small T antigen is oncogenic in transgenic mice. J. Invest. Dermatol. 2015;135(5):1415–24
Visvader JE. Cells of origin in cancer. Nature. 2011;469(7330):314–22
Walsh NM. Primary neuroendocrine (Merkel cell) carcinoma of the skin: morphologic diversity and implications thereof. Hum. Pathol. 2001;32(7):680–9
Wang K, Li M, Hakonarson H. ANNOVAR: functional annotation of genetic variants from high-throughput sequencing data. Nucleic Acids Res. 2010;38(16):e164
Woo S-H, Stumpfova M, Jensen UB, Lumpkin EA, Owens DM. Identification of epidermal progenitors for the Merkel cell lineage. Dev. Camb. Engl. 2010;137(23):3965–71
Xiao Y, Thoresen DT, Williams JS, Wang C, Perna J, Petrova R, et al. Neural Hedgehog signaling maintains stem cell renewal in the sensory touch dome epithelium. Proc. Natl. Acad. Sci. U. S. A. 2015;112(23):7195–200
Zur Hausen A, Rennspiess D, Winnepenninckx V, Speel E-J, Kurz AK. Early B-cell differentiation in Merkel cell carcinomas: clues to cellular ancestry. Cancer Res. 2013;73(16):4982–7

Legends

Figure 1. Microscopic and immunohistochemical features of the trichoblastoma/MCC combined tumor. (a) Morphological features of the case (hematein-phloxin-saffron staining (HPS))**.** Low magnification revealed a well delimitated tumor mainly located in the subcutis without connection to the epidermis (bar=1 mm); higher magnification shows the MCC in close association with the trichoblastoma (TB; bar=250 μm). Indeed, the trichoblastoma was composed of clusters and anastomotic strands of basaloid epithelial cells surrounded by a clear stroma containing mucin deposits whereas the MCC was characterized by sheets of small to medium sized cells with scant cytoplasm, round nucleus, dusty chromatin, and a high mitotic rate. (**b-e)** Microscopic and immunohistochemical details of the case (bar=100 μm).

Two regions from the trichoblastoma part, representing either the majority of TB area without LT expression (LT(-) TB) or an TB area with occasional LT expression (LT(+) TB), as well as one representative region from the MCC part are displayed. In the LT-positive area of the trichoblastoma, a population of clear cells with coarse chromatin morphologically distinct from the other cells of the trichoblastoma but also from the MCC tumor cells (black arrows) was evident in the HPS staining. While KRT20 stained with a diffuse pattern in virus-negative parts of the trichoblastoma, in MCPyV-LT-expressing areas a KRT20 dot-like pattern was observed comparable to MCC. The LT expressing area was additionally characterized by an increased number of SOX2-expressing cells compared to the rest of the trichoblastoma, while the MCC cells generally displayed nuclear positivity for this marker.

Figure 2. The MCC part of the combined tumor fulfills the hallmarks of MCPyV-positive MCC. (a) Integration of MCPyV in chromosome 3 of the MCC genome. DNA isolated from the MCC part of the combined tumor was analyzed by whole genome sequencing (WGS) and confirmed by Sanger sequencing. The integration break points in the viral genome (Genbank EU375803) as well as in chromosome 3 (GRCh37; NC000003.11) are depicted. To note, human sequences adjacent to the integration break points were found to be swapped. Moreover, sequencing revealed a deletion in the viral genome (Δ2248-2542). Frequently, MCPyV integrates as head to tail concatemer. In this case, nucleotides 1557-1956 are followed by one or more full length copies (1957-1956) which is predicted to lead to (**b)** one or two different truncated Large T antigen proteins expressed in the MCC part. One premature stop codon is caused by the integration break point at nucleotide 1956 in the final MCPyV genome of the concatemer and will lead to expression of the 443 N-terminal amino acids of LT followed by 3 additional amino acids. A second larger truncated LT is encoded in case that the concatemer encompasses more than two full copies of the MCPyV genome. The Δ2248-2542 deletion leads to an LT sequence coding for the 540 N-terminal amino acids

followed by three frame shifted amino acid codons prior to a stop codon. (**c)** PCR was performed with primers for general MCPyV detection (MCPyV; product size = 84 bp), flanking Δ2248-2542 (Δ region), or for the 5' (5' integ.; product size = 171 bp) and 3' (3' integ.; product size = 172 bp) integration sites, respectively. For MCPyV wt the Δ region PCR will produce a PCR product of 398 bp, while it will be only 103 bp when the MCPyV contains the deletion. Notice a faint band for the 5' integration site with DNA from the trichoblastoma part at around 200 bp. Sanger sequencing, however, confirmed it to be an unspecific product.

Figure 3. Trichoblastoma and MCC cells of the combined tumor share six protein-altering somatic variants. Whole exome sequencing identified six variants shared by trichoblastoma and MCC (**Supplementary Table S2**). The variant as well as the allelic frequency for the alternative sequence (alt.) derived from the massive parallel sequencing are given in the figure. DNA obtained from PBMC or any of the two tumor components were amplified by primers specific for the respective variants. The results of the direct sequencing are depicted. Blue shading indicates the position of the variant or the frame shift region caused by deletion, respectively.

Figure 4. Shared morphologic and immunohistochemical features of MC progenitors in the hair follicle and trichoblastoma cells. Overview photographs (bar = 1 mm) of the complete specimen containing the combined TB/MCC and a hair follicle as well as details of each component (bars = 100 mm) are displayed. (**a)** Morphological examination (hematein-phloxin saffron (HPS) staining) revealed clusters of basaloid cells displaying focal palisading in the trichoblastoma periphery, similar to the germinative cells of the hair follicle. In line with these findings, expression of **(b)** KRT15, a marker expressed by the outer root sheath of the hair follicle, was observed also in the trichoblastoma periphery. Furthermore, in TB as

well as in the hair follicle cells, the progenitor markers **(c)** KRT17 and **(d)** SOX9 are frequently present. The same applies to nuclear localization of GLI1 **(e)** indicating activation of the sonic hedgehog pathway which is known to be critical for the maintenance of MC progenitors and their subsequent MC differentiation. In accordance with the presence of many markers indicating MC differentiation capability in the hair follicle and TB KRT20-positive MCs **(f)** can be found in both tissues.

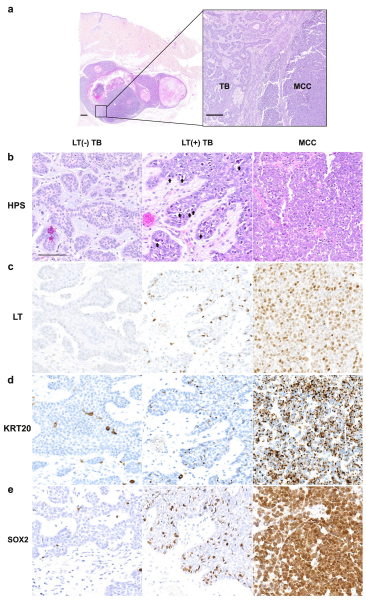

Figure 1. Microscopic and immunohistochemical features of the trichoblastoma/MCC combined tumor.
(a) Morphological features of the case (hematein-phloxin-saffron staining (HPS)). Low magnification revealed a well delimitated tumor mainly located in the subcutis without connection to the epidermis (bar=1 mm); higher magnification shows the MCC in close association with the trichoblastoma (TB; bar=250 µm). Indeed, the trichoblastoma was composed of clusters and anastomotic strands of basaloid epithelial cells surrounded by a clear stroma containing mucin deposits whereas the MCC was characterized by sheets of small to medium sized cells with scant cytoplasm, round nucleus, dusty chromatin, and a high mitotic rate. (b-e) Microscopic and immunohistochemical details of the case (bar=100 µm). Two regions from the trichoblastoma part, representing either the majority of TB area without LT expression (LT(-) TB) or an TB area with occasional LT expression (LT(+) TB), as well as one representative region from the MCC part are displayed. In the LT-positive area of the trichoblastoma, a population of clear cells with coarse chromatin morphologically distinct from the other cells of the trichoblastoma but also from the MCC tumor cells (black arrows) was evident in the HPS staining. While KRT20 stained with a diffuse pattern in virus-negative parts of the trichoblastoma, in MCPyV-LT-expressing areas a KRT20 dot-like pattern was observed comparable to MCC. The LT expressing area was additionally characterized by an increased number of SOX2-expressing cells compared to the rest of the trichoblastoma, while the MCC cells generally displayed nuclear positivity for this marker.

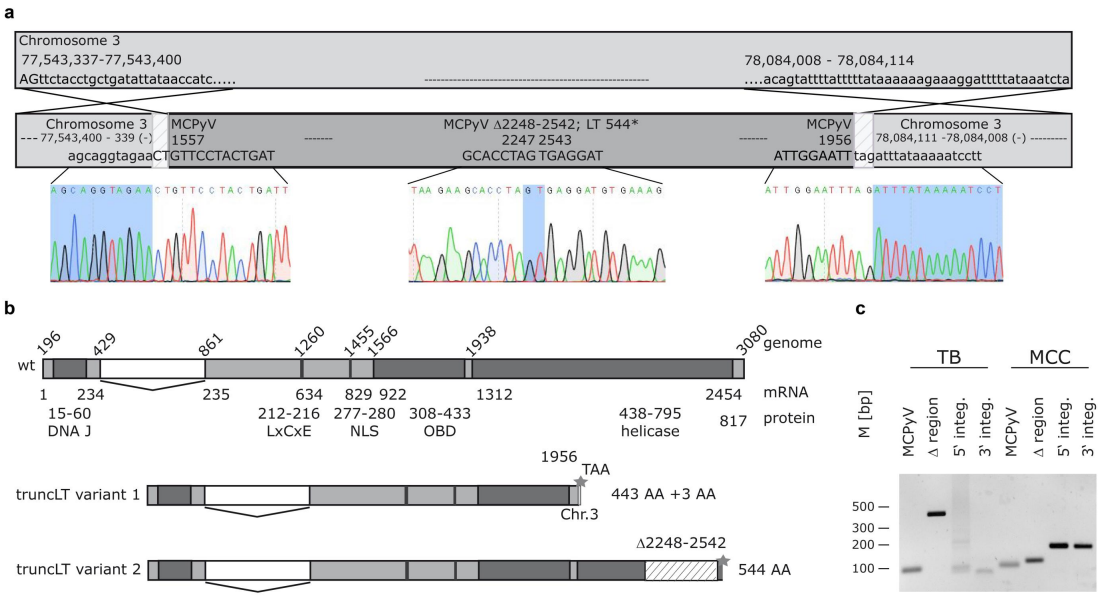

Figure 2. The MCC part of the combined tumor fulfills the hallmarks of MCPyV-positive MCC. (a) Integration of MCPyV in chromosome 3 of the MCC genome. DNA isolated from the MCC part of the combined tumor was analyzed by whole genome sequencing (WGS) and confirmed by Sanger sequencing. The integration break points in the viral genome (Genbank EU375803) as well as in chromosome 3 (GRCh37; NC000003.11) are depicted. To note, human sequences adjacent to the integration break points were found to be swapped. Moreover, sequencing revealed a deletion in the viral genome (Δ2248-2542). Frequently, MCPyV integrates as head to tail concatemer. In this case, nucleotides 1557-1956 are followed by one or more full length copies (1957-1956) which is predicted to lead to (b) one or two different truncated Large T antigen proteins expressed in the MCC part. One premature stop codon is caused by the integration break point at nucleotide 1956 in the final MCPyV genome of the concatemer and will lead to expression of the 443 N-terminal amino acids of LT followed by 3 additional amino acids. A second larger truncated LT is encoded in case that the concatemer encompasses more than two full copies of the MCPyV genome. The Δ2248-2542 deletion leads to an LT sequence coding for the 540 N-terminal amino acids followed by three frame shifted amino acid codons prior to a stop codon. (c) PCR was performed with primers for general MCPyV detection (MCPyV; product size = 84 bp), flanking Δ2248-2542 (Δ region), or for the 5' (5' integ.; product size = 171 bp) and 3' (3' integ.; product size = 172 bp) integration sites, respectively. For MCPyV wt the Δ region PCR will produce a PCR product of 398 bp, while it will be only 103 bp when the MCPyV contains the deletion. Notice a faint band for the 5' integration site with DNA from the trichoblastoma part at around 200 bp. Sanger sequencing, however, confirmed it to be an unspecific product.

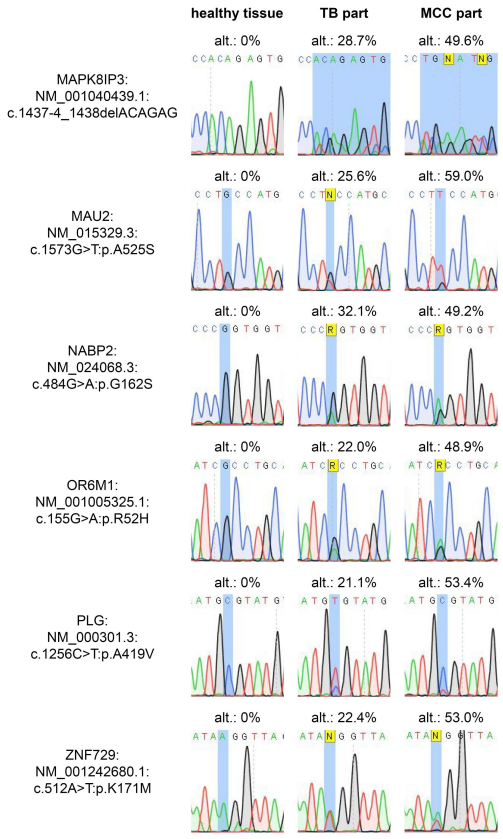

Figure 3. Trichoblastoma and MCC cells of the combined tumor share six protein-altering somatic variants. Whole exome sequencing identified six variants shared by trichoblastoma and MCC (Supplementary Table S2). The variant as well as the allelic frequency for the alternative sequence (alt.) derived from the massive parallel sequencing are given in the figure. DNA obtained from PBMC or any of the two tumor components were amplified by primers specific for the respective variants. The results of the direct sequencing are depicted. Blue shading indicates the position of the variant or the frame shift region caused by deletion,